Molecular Crystals and Liquid Crystals Science and Technology. Section A. Molecular Crystals and Liquid Crystals

Publication details, including instructions for authors and subscription information:
http://www.tandfonline.com/loi/gmcl19

Vibrational Modes in C_{60} and C_{60} Polymer

P. C. Eklund [a], A. M. Rao [a], Ping Zhou [a], Ying Wang [a], Kai-An Wang [a], J. M. Holden [a], M. S. Dresselhaus [b] & G. Dresselhaus [c]

[a] Department of Physics and Astronomy, Center for Applied Energy Research University of Kentucky, Lexington, Kentucky, 40506

[b] Department of Physics and Department of Electrical Engineering and Computer Science, Massachusetts Institute of Technology, Massachusetts, 02139

[c] Francis Bitter National Magnet Laboratory, Massachusetts Institute of Technology, Massachusetts, 02139

Version of record first published: 04 Oct 2006.

To cite this article: P. C. Eklund , A. M. Rao , Ping Zhou , Ying Wang , Kai-An Wang , J. M. Holden , M. S. Dresselhaus & G. Dresselhaus (1994): Vibrational Modes in C_{60} and C_{60} Polymer, Molecular Crystals and Liquid Crystals Science and Technology. Section A. Molecular Crystals and Liquid Crystals, 256:1, 199-208

To link to this article: http://dx.doi.org/10.1080/10587259408039248

Mol. Cryst. Liq. Cryst. 1994, Vol. 256, pp. 199–208
Reprints available directly from the publisher
Photocopying permitted by license only

VIBRATIONAL MODES IN C_{60} AND C_{60} POLYMER

P. C. EKLUND,[1] A. M. RAO,[1] PING ZHOU,[1] YING WANG,[1] KAI-AN WANG,[1] J. M. HOLDEN,[1] M. S. DRESSELHAUS[2] and G. DRESSELHAUS[3]
[1] Department of Physics and Astronomy and Center for Applied Energy Research
University of Kentucky, Lexington, Kentucky 40506.
[2] Department of Physics and Department of Electrical Engineering and Computer Science,
Massachusetts Institute of Technology, Massachusetts 02139.
[3] Francis Bitter National Magnet Laboratory,
Massachusetts Institute of Technology, Massachusetts 02139.

Abstract The vibrational properties of oxygen-free C_{60} films indicate the nearly ideal molecular nature of solid C_{60}. Numerous sharp Raman lines (~98) and infrared lines (~98) were observed and assigned to first-order modes, or combination and overtone intramolecular mode frequencies of C_{60}. Analysis of these vibrational modes yields a complete, self-consistent set of the 46 fundamental intramolecular mode frequencies of a C_{60} molecule. Irradiation of oxygen-free C_{60} films with visible or ultraviolet light phototransformed C_{60} to a new polymeric phase. We present experimental evidence which suggests the formation of covalent C-C bonds between C_{60} molecules in the polymeric phase. Furthermore, the rate for thermal dissociation of these intermolecular bonds is found to follow an Arrhenius' type behavior with an activation energy E_a = 1.25 eV. Our experimental results will also be compared to recent theoretical calculations and connected with the photophysical behavior of C_{60}.

INTRODUCTION

The discovery by Smalley, Kroto and co-workers[1] of new carbon cage molecules C_N referred to as *"fullerenes"* has led to a new class of carbon-based solids which exhibit a wide variety of unusual physical and chemical properties[2-4]. In this paper, we review some of our recent work on the vibrational properties of pristine C_{60} and photopolymerized solid C_{60} films. First, we will present the results obtained from the first- and higher-order Raman scattering[5-7] and infrared (IR) studies[8] of pristine C_{60} films. Next, we discuss results of our studies on the photopolymerization of solid C_{60}[9-13].

I. VIBRATIONAL SPECTRUM OF C_{60} FILMS

As is now well known, pristine solid C_{60} is a van der Waals-bonded molecular solid whose electronic and vibrational properties are strongly connected to the properties of the molecule itself, which exhibits icosahedral (I_h) symmetry. This symmetry, which can be identified with the pattern of periodically placed, 20 hexagonal and 12 pentagonal faces on a soccer ball (inset figure in Fig. 1), is quite high, and this leads to a dramatic simplification of the vibrational and electronic states. Several experiments on pristine C_{60} indicate that below T_o ~260 K, the C_{60} molecules in the solid undergo an orientational ordering[4, 14-17]. The data have been interpreted to indicate that (1) for $T > T_0$, the C_{60} molecules spin freely about

randomly oriented axes on fcc lattice positions, and (2) for $T < T_0$, two of the three rotational degrees of freedom in the high T phase are lost, and the molecules undergo a "ratchet-like" orientational hopping about four specific (111) directions, as determined by x-ray[14, 18] and neutron[15, 19] studies. At T=90K, a second transition to a merohedrally disordered glass phase (MDGP) occurs[14,15] leading to an estimate of the number of molecules oriented such that an electron-rich double bond on one molecule faces the electron-deficient opening in a pentagon (~83%) or hexagon (~17%) of the adjacent molecule.

For an isolated C_{60} molecule, out of the 180-6 = 174 intramolecular vibrational modes, only 46 distinct mode frequencies are possible[20, 21]. Ten ($8H_g + 2A_g$) of these 46 modes are Raman-active and four ($4F_{1u}$) are IR-active modes[21] and have been determined experimentally by the first-order Raman and IR spectroscopies[20, 22, 23]. Figure 1 shows the IR and Raman spectra obtained at room temperature on thin oxygen-free solid films of C_{60}, vacuum deposited onto various substrates, e.g. Si(100), KBr and fused quartz[20]. The IR spectrum (A) in Fig. 1, shows four prominent narrow lines at 526, 576, 1182 and 1428 cm^{-1} that are associated with the $4F_{1u}$ intramolecular modes and in spectrum (B), ten of the twelve features are identified with the Raman allowed $2A_g$ (493 and 1469 cm^{-1}) and $8H_g$ vibrations[9]. All the carbon atom displacements in the 493 cm^{-1} A_g symmetric breathing mode are in the radial direction and are of equal magnitude. The A_g mode at 1469 cm^{-1} corresponds to tangential displacements of the 5 carbon atoms around each of the 12 pentagons and, therefore, is also called the "pentagonal pinch" (PP) mode.

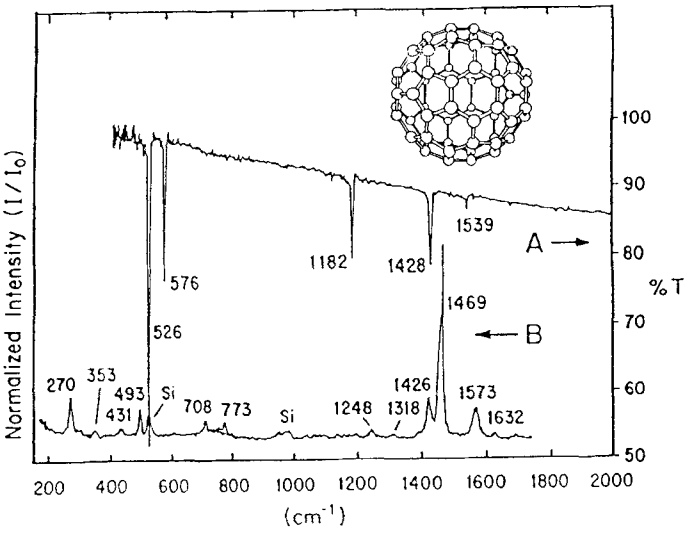

Fig. 1: Fourier transform infrared (FTIR) transmission (spectrum A) and Raman spectra (spectrum B) of pristine C_{60} film. The Raman spectra were taken at low laser power density (< 50 mW/mm^2) using the 488 nm Ar ion line on samples deposited on fused quartz substrates. FTIR samples were deposited on KBr substrates. Inset: Each carbon atom is at an equivalent position on the corners of a regular truncated icosahedron with 20 hexagonal and 12 pentagonal faces.

As will be discussed in section II, solid C_{60} is sensitive to visible and ultraviolet (UV) radiation,

being easily phototransformed at room temperature from a weakly bonded van der Waals solid to a polymeric $(C_{60})_N$ phase in which N C_{60} molecules are cross-linked via covalent bonds[9-13]. For $T < T_c$, the relative orientation of adjacent C_{60} molecules in the lattice does not satisfy the topochemical requirements for the formation of the cross-linking covalent bonds[11] and therefore, it is possible to expose the C_{60} films to sufficiently high laser excitation intensities to study numerous weaker features (overtones and combination modes) in the Raman spectrum in detail, without polymerizing or inflicting photoinduced damage to the C_{60} films. Furthermore, above the range of significant thermal decomposition temperature (T_p ~450 K) for the photopolymerized C_{60} films, the fullerene molecules are spinning rapidly about their fcc lattice positions and any photoinduced dimers [C_{60}=C_{60}] that might be formed by the Raman laser will immediately be thermally decomposed[13]. Group theoretical analysis of the combination and overtone mode frequencies provides an opportunity to determine the mode frequencies and symmetries of some of the optically "silent" vibrational modes (A_u, F_{1g}, F_{2g}, G_g, G_u and H_u). Besides the 14 ($4F_{1u}$+ $2A_g$ +8 H_g) first-order allowed IR and Raman modes (Fig. 1), at least additional 98 weak Raman lines (Fig. 2) and 98 weak IR lines (Fig. 3) can be observed in the spectra obtained from thick (~1-4 μm) C_{60} films. Raman spectra at temperatures T = 20 K and 523 K for solid C_{60} films (~7000 Å) are shown in Fig. 2. We find that many of the strongest second-order Raman lines involve only modes which are also observed in first-order. These special second-order modes have been marked on Fig. 2 and account well for most of the intense second-order Raman features above ~1000 cm^{-1}.

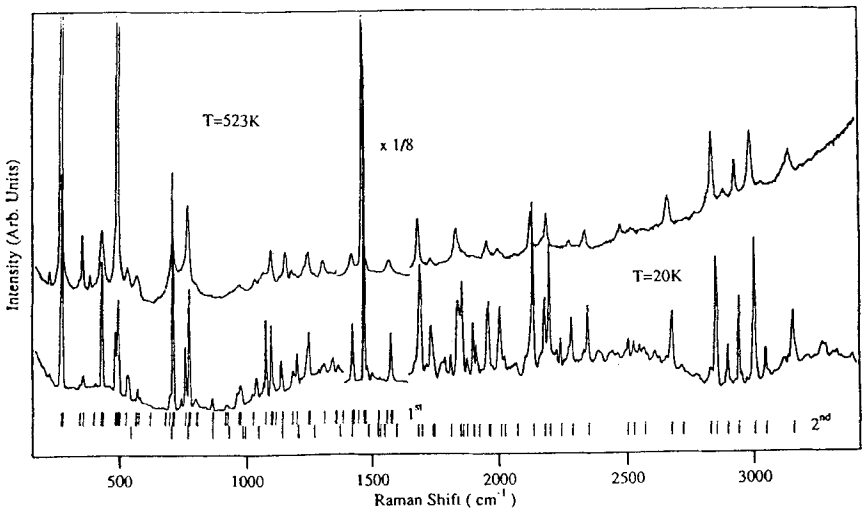

Fig. 2: Raman spectra for a solid C_{60} film (d ~7000 Å) taken at T= 523 K and 20 K using 488 nm Ar ion laser radiation. The mode frequencies shown schematically in the figure are as follows: (upper, marked first) gives the position of all 46 fundamental frequencies and the Raman-allowed modes are marked as darker ticks, and (lower, marked second) gives the position of all overtone and combination modes.

Somewhat weaker features in the Raman spectra might be expected to arise from combination modes where only one of the components relates to first-order Raman-active lines.

In principle, the second-order IR spectrum could also provide a method for determining the frequencies of the optically silent modes. The observation of additional second order IR lines in Fig. 3 suggests, on the basis of the group theoretical arguments[8], that certain modes (Γ_i) which are silent in first order are also playing a role in the second-order IR spectrum. Narrow structure associated with various first and higher order vibrational modes are superimposed on a background exhibiting broad, large amplitude oscillations (~500 cm^{-1} period). These oscillations are due to an interference between beams suffering various multiple internal reflections inside the C_{60} film[24]. Since the A_g and H_g modes are known from first-order Raman spectroscopy[20, 22], it is only the silent modes that are not as well determined. By adjusting the frequencies of the silent modes together with the known frequencies for the A_g, H_g and F_{1u} modes, we have obtained the 46 distinct mode frequencies for a C_{60} molecule and can be found in Ref. [8]. Finally, it should be mentioned that the silent modes can also be activated by isotopic substitution (i.e. $^{13}C^{12}C_{59}$: each of these molecules contains one ^{13}C and 59 ^{12}C atoms), as was previously reported in benzene[25]. Several of the weaker features observed in Figs. 2 and 3 are identified with isotopic activation of silent modes[8].

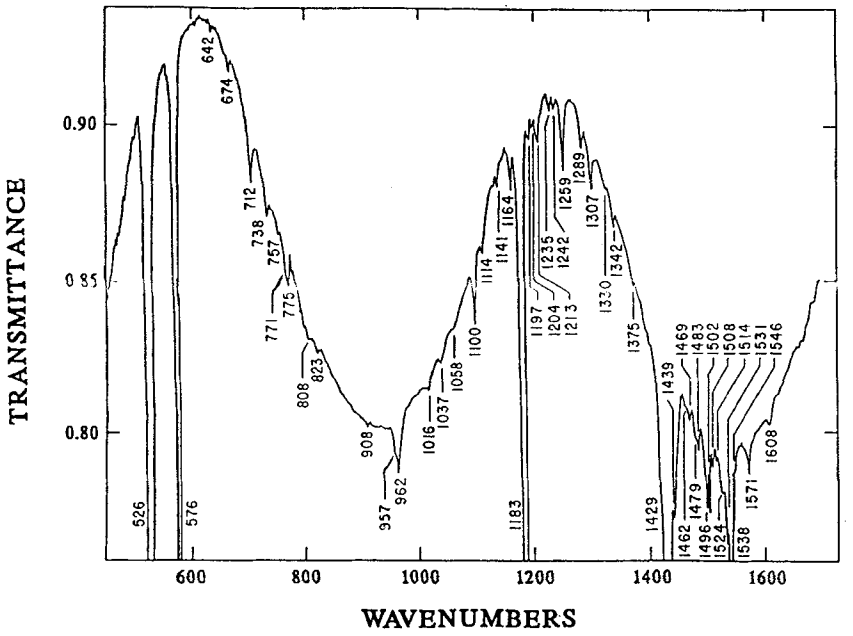

Fig. 3: Infrared transmission spectrum of a C_{60} film (d~ 4μm) vacuum deposited on a KBr substrate. The large periodic oscillations are due to a Fabry-Perot interference effect in the C_{60} film.

II. PHOTOINDUCED POLYMERIZATION OF C_{60}

In this section, we present experimental results which indicate that the application of visible or ultraviolet

light to solid C_{60} polymerizes the structure, linking the molecules together in a covalently bonded structure. Previously, on the basis of Raman scattering studies, we reported the observation that Ar ion laser radiation at 514.5 and 488.0 nm exceeding ~50 mW/mm^2 appeared to initiate a photoinduced transformation of an oxygen-free, fcc C_{60} to a different solid phase with a richer Raman spectrum[20, 26]. In particular, the high frequency A_g-symmetry "pentagonal-pinch" (PP) mode was observed to broaden and downshift at room temperature from 1469 cm^{-1} to ~1460 cm^{-1}, while the polarization ratio for this mode deteriorated from 100% in pristine C_{60} to ~80% in the phototransformed phase[20, 26]. Similar downshifting of the PP mode was also observed when oxygen-free C_{60} films were irradiated with UV-visible light using a 300 W Hg arc source[9]. There has been some disagreement in the literature about the value of the PP mode frequency. In our opinion, the value 1469 cm^{-1} has been incorrectly associated with only oxygen-contaminated C_{60}[27-30]. Fourier transform Raman studies by Chase *et al.*[31] using a YAG laser with photon energy (1.06 eV), less than the absorption threshold in C_{60}[32, 33], confirm the 1469 cm^{-1} PP mode frequency for oxygen-free, fcc C_{60} obtained using a low power Ar ion laser beam[20, 26]. Furthermore, unlike pristine C_{60}, the phototransformed C_{60} films were found to be insoluble in toluene, suggesting that the weak van der Waals bonding between the neighboring C_{60} molecules has been altered by the UV-visible irradiation[9].

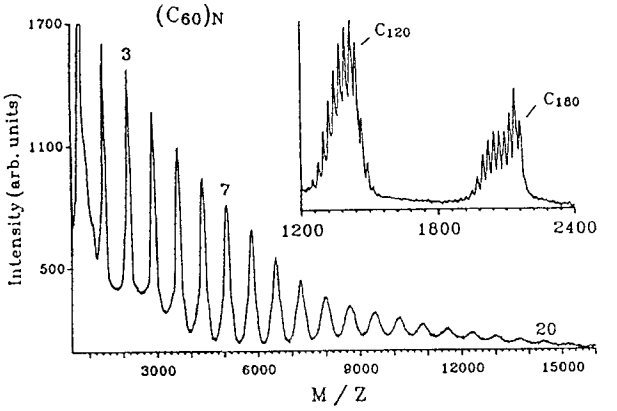

Fig. 4: Laser desorption mass spectrum of C_{60} exposed to radiation from an unfiltered mercury arc of power 300 W. Each peak corresponds to a mass m = 12 X 60 X N a.m.u., where N =1,2, ..20. Inset: LDMS spectrum shown on an expanded scale in the region of the dimer (C_{120}) and trimer (C_{180}), indicating C_2 loss and gain in the desorption process.

In Fig. 4, we display a laser desorption mass spectroscopy (LDMS) spectrum collected on a *phototransformed* film (d= 2000 Å , 12 hr exposure to radiation from a 300 W Hg arc lamp). The mass range encompasses C_{60} (720 amu) up to 21 x C_{60} (15120 amu). The spectrum in Fig. 4 was taken using the following desorption conditions : ~10^{-7} Torr vacuum, pulsed N_2 laser at 337 nm focused to a spot size of 0.3 mm dia., 5 to 10 ns pulse width, pulse energy 10 mJ/cm^2 , and 10 Hz pulse repetition rate. A succession of 20 clear peaks is evident in the mass spectrum of Fig. 4, which were identified with

clusters of cross-linked fullerene molecules $(C_{60})_N$ [9, 10]. In the inset to Fig. 4, the data in the vicinity of C_{120} (dimer) and C_{180} (trimer) are displayed on an expanded scale, and the C_2 structure is clearly evident. On the other hand, the LDMS spectrum of a *pristine* film was observed to exhibit a series of mass peaks out to N=5[9, 10]. This suggests that at high laser power, the N_2 desorption laser itself is capable of producing polymerized C_{60}. For comparison to this latter result, the pristine film under the reduced (laser power) desorption conditions exhibited only the N=1 peak in its LDMS spectrum[10]. Other evidence subsequently found in support of a polymeric form of C_{60} include photoelectron spectroscopy of C_{60} films that were irradiated with UV light[34], and IR spectroscopy of solid C_{60} that were subjected to high pressures[35].

In Fig. 5 we show the effect of the phototransformation (or polymerization) on the vibrational modes of solid C_{60}. Room temperature IR transmission and Raman spectra for phototransformed C_{60} films are shown. In contrast to vibrational spectra of the pristine C_{60} fcc phase (see Fig. 1), the Raman and IR spectra of the phototransformed phase exhibit many more lines, indicating that the icosahedral symmetry of the C_{60} molecule has been lowered, consistent with the proposed photopolymerization process. Polymerization in C_{60} can also be induced by pressure[35]. Using IR spectroscopy as a probe, Yamawaki *et al.*[35] observed additional weak lines similar to those shown in Fig. 5 (spectrum C) when the sample was subjected to high pressure (7 GPa). The origin of these weak additional lines was attributed to the pressure-induced formation of the C_{60} polymer[35]. Furthermore, in the polymerized C_{60} films, a new Raman-active mode was observed at ~118 cm^{-1} which is identified with the stretching of these cross-linking bonds[9, 13] and molecular dynamics calculations for the C_{60} dimer report this interball mode at 104 cm^{-1}[36].

Next, we discuss the photoinduced mechanism we proposed for the formation of the covalent cross-linking bonds in the phototransformed C_{60} films. As shown in Fig. 6, Raman spectra of a C_{60} film (d~

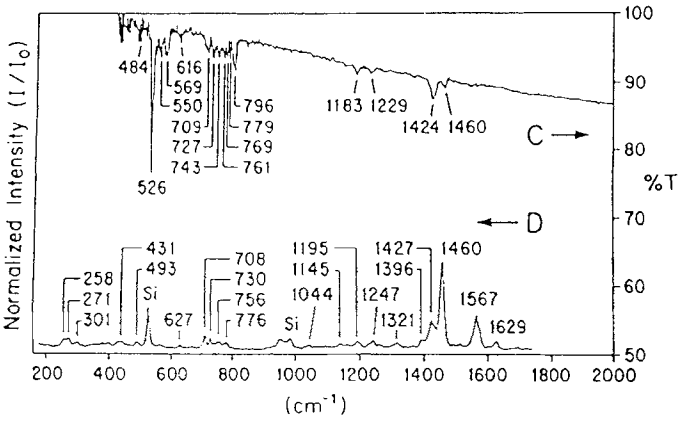

Fig. 5: Fourier transform infrared (FTIR) transmission (spectrum C) and Raman spectra (spectrum D) of phototransformed C_{60} film.

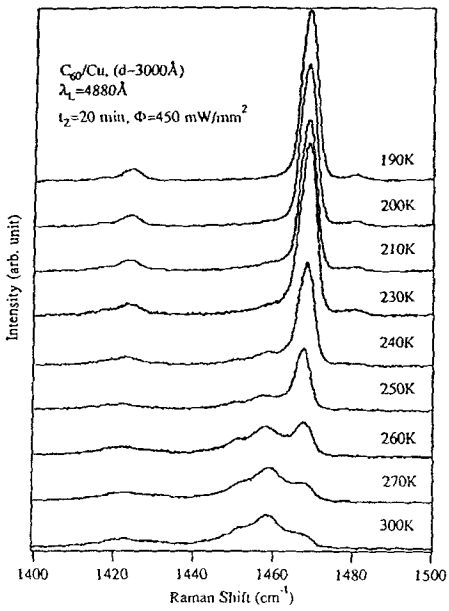

Fig. 6: Raman spectra of a C_{60} film (d~ 3000 Å) on a Cu substrate as a function of temperature (T) collected after 20 min. pre-exposure to 488 nm laser irradiation.

3000 Å) deposited on a polished Cu substrate were collected at various temperatures (190 K < T < 300 K) using a fixed grating angle, a cooled, charge-coupled-array-detector, and 488 nm radiation from an Argon ion laser. The Raman laser also served as the source to promote the phototransformation of the C_{60} film. For T ≤ 250 K, the existence of a dominant 1469 cm^{-1} Raman peak, indicative of pristine C_{60}[20], is observed despite the 20 min pre-exposure to high laser fluence. Little or no evidence for phototransformation is detected, i.e., the *unpolarized, photo-induced* ~1458 cm^{-1} mode is weak or absent altogether, indicating the film is effectively resisting photopolymerization in this temperature range[20]. With increasing T above a threshold near 250 K, the film photopolymerizes more rapidly, evidenced by the rapid growth of the 1458 cm^{-1} Raman structure. The threshold for the photopolymerization near ~250 K is clearly evident, and this temperature is close to the orientational ordering temperature.

The "2+2 cycloaddition" mechanism is a well known photochemical reaction resulting in the covalent attachment of adjacent molecules[37]. This mechanism is active in molecular solids when carbon double bonds on each adjacent molecules are oriented parallel to one another and separated by less than ~4.2 Å [37]. By photochemical assistance, an excited molecular state is formed, and as a result both these double bonds are broken and reform as a four sided ring (Fig. 7c). Two C_{60} molecules might dimerize by the "2+2 cycloaddition" mechanism as shown in Fig. 7d. Since a C_{60} molecule contains 30 reactive double bonds tangential to the ball surface, and these double bonds on adjacent molecules can be separated by as little as 3.5 Å in pristine solid C_{60}[14], then solid C_{60} can be seen to satisfy the general topochemical requirement for "2+2 cycloaddition" in a constrained medium [37], *but only for* $T > T_0$. At low T, the double bonds on adjacent molecules avoid each other (Fig. 7a and 7b), and according to the topochemical requirement, the reaction should be suppressed. For $T > T_0$, however, the freely spinning molecules enjoy 30(30) = 900 favorable orientations to promote the "2+2 cycloaddition" reaction.

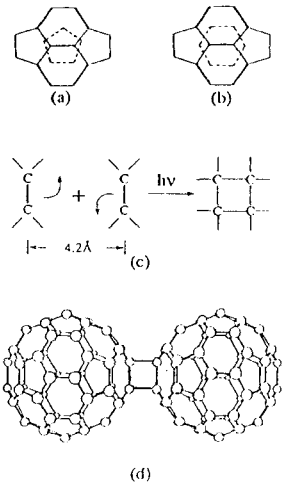

Fig. 7: (a) and (b) : Two possible orientations of adjacent C_{60} molecules in the MDGP. (c): Schematic "2 + 2 cycloaddition" reaction between parallel carbon double bonds on adjacent molecules. (d): A C_{60} dimer produced by a photoinduced "2 + 2 cycloaddition" reaction.

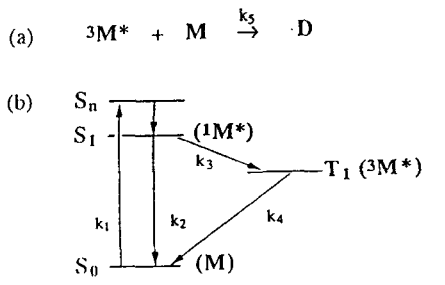

Fig. 8: (a) Bimolecular photochemical reaction in which a C_{60} monomer in the excited triplet state ($^3M^*$) reacts with a monomer in the ground state (M) to form a dimer (D). (b) Schematic energy level diagram for the C_{60} monomer, showing the principal levels involved. The k_i are the respective rate constants, and the other symbols are described in the text.

Furthermore, the photophysics of C_{60} also seems to favor the proposed "2+2 cycloaddition" reaction mechanism. First, strong, dipole-allowed, singlet-singlet absorption is observed above ~2.3 eV[38]; second, a ~100% efficient intersystem crossing[39, 40] is needed to populate significantly the first excited triplet state (T_1); and third, a sufficiently long T_1 lifetime (~40 μsec[39]) is needed to maintain a significant number of molecules in the reactive triplet state. In kinetics studies which we discuss below, we find that the rate limiting step in the photodimerization process is the photoexcitation of the monomer to excited singlet state S_n[12], i.e., one dimer is found for very 488 nm photon absorbed. This result follows directly from the ~100% efficient intersystem crossing.

Another experimental result consistent with the importance of the T_1 state in the dimerization pathway is the observation that intercalated dioxygen "hardens" C_{60} against phototransformation, i.e., high laser flux was not observed to produce phototransformation when dioxygen was present in the lattice [20, 26, 41]. The stabilizing influence of dioxygen is undoubtedly connected with the reported quenching of the C_{60} (T_1) state via an interaction with the $(O_2)\ ^3\Sigma$ state [40], thereby suppressing photopolymerization.

Finally, we discuss the kinetics of the photoinduced polymerization of C_{60} films deduced from the time evolution of Raman spectrum in the vicinity of 1469 cm^{-1} mode. The C_{60} film was exposed at T = 300 K to photon flux $\Phi_0 \sim 8.3$ mW/mm^2 at 488 nm from an Argon ion laser. This irradiation level was chosen to both slowly phototransform the film, as well as to stimulate the Raman spectrum. A least-squared Lorentzian lineshape analysis of the Raman spectra was used to determine the relative concentration of the C_{60} monomers M(t) (integrated area under the 1469 cm^{-1} line) and dimers D(t) (integrated area under the ~1459 cm^{-1} line) as a function of time t. Details regarding the lineshape analysis

and the experiment is reported in Ref. [12]. Initially, a single line is observed at 1469 cm^{-1} which is 100% polarized[26] and identified with the "pentagonal pinch" mode (A_g) of pristine C_{60}. Early in this phototransformation process dimers, and later, trimers, etc., form, eventually leading to the polymeric phase $(C_{60})_N$. The progression from the pristine film to one containing dimers can be monitored by the shift in spectral weight from the 1469 cm^{-1} line to the ~1459 cm^{-1} line. After ~600 minutes, the phototransformation to the polymer is complete, and the 1469 cm^{-1} line is absent from the Raman spectrum[12] indicating the formation of cross linking C-C bonds between C_{60} molecules via a "2+2" cycloadditon mechanism discussed above[11].

Using the molecular energy level diagram presented in Fig. 8, the kinetics of the photoinduced polymerization in solid C_{60} can be understood from a conventional triplet state photochemical mechanism, where a monomer in the excited triplet state ($^3M^*$) reacts with a monomer in the ground state (M) to yield the dimer (D), i.e., $^3M^* + M \rightarrow D$; this reaction is assumed to proceed as a normal bimolecular reaction with rate constant k_5 (Fig. 8a). Rate constants k_i (i = 1-4) are required to describe the rate at which $^3M^*$ molecules can be produced per incident photon (Fig. 8b). First, the system must be excited by optically pumping the monomer to excited singlet states S_j, where the pumping rate constant k_1 depends on the incident light flux Φ_0. The S_j states then usually decay very rapidly to S_1[42], so we ignore the internal conversion rate constants for $S_j \rightarrow S_1$. Once the system is in S_1 (or $^1M^*$), it can return to the ground state S_0 (or M) by radiative recombination (k_2). However, the singlet exciton recombination has a low quantum yield (~ 0.07% [43]), therefore, the system decays to T_1 (or $^3M^*$) by a nearly 100 % efficient intersystem crossing ($k_3 \sim 3 \times 10^{10}$ s^{-1} [44]). Finally, $^3M^*$ can return either to the monomeric ground state M via k_4, or the $^3M^*$ state can undergo a bimolecular reaction with M (k_5) to form the dimer D. The coupled set of equations which describe the time evolution of this system are[13] :

$$M(t) \approx (M_0) \exp(-2k_1t) \quad \text{and} \quad D(t) \approx (1/2)(M_0)\,(1-\exp(-2k_1t)), \qquad (1)$$

where M_0 is the initial density of monomers. From the form of these solutions it can be seen that the optical pumping (rate k_1) must be the rate limiting step, and one absorbed photon produces one dimer.

In-situ temperature dependence of the Raman spectrum for an initially photopolymerized C_{60} film in the vicinity of the symmetric "pentagonal pinch mode" shows that the C_{60} polymer can be driven back towards pristine, van der Waals bonded C_{60} solid. Details regarding the thermal decomposition of the C_{60} polymer are available elsewhere[13]. A least squares Lorentzian lineshape analysis was carried out to determine values for the T-dependence of the integrated intensity (I), frequency (ω) and linewidth (Γ) for the 1469 cm^{-1} (pristine C_{60}) and 1459 cm^{-1} (C_{60}-polymer) lines. Below ~100 °C, the linear increase of Γ_{1459} was assigned to thermal broadening[13]. However, above ~100 °C, Γ_{1459} exhibited an anomalous decrease with increasing temperature, which is interpreted as evidence that the polymer has dissociated to a solid containing primarily monomers and dimers (i.e., for T > 100 °C, the contribution to Γ from inhomogeneous broadening decreases). Assuming a fixed number density of C_{60} shells (M_0), and under steady state conditions, when the system is dominated by monomers and dimers, the intensity ratio I_{1459}/I_{1469} was shown to be proportional to the inverse thermal decomposition rate $(k_T)^{-1}$. Anticipating

an exponential temperature dependence (i.e. Arrhenius' behavior) for k_T (i.e., $k_T = A \exp(-E_a/k_BT)$, where k_B is Boltzmann's constant and A is a pre-exponential constant with units 1/time), a plot of $\log_{10}(I_{1459}/I_{1469})$ vs. $1/k_BT$, showed a nearly linear relationship over the entire temperature range where reliable intensity information can be obtained [13]. A linear fit to the data results in the activation energy E_a = 1.25 eV [13]. We suggest that the observed linear behavior of the ratio I_{1459}/I_{1469}, over the larger T-range as evidence that the thermal energy required to dissociate a monomer from all other oligomers is approximately the same as that needed to dissociate a dimer into two monomers. Therefore, we interpret the 1.25 eV activation energy obtained from the fit to the data as the thermal energy required to dissociate a monomer from any oligomer in C_{60}-polymer.

ACKNOWLEDGEMENTS

The research at UK was supported in part by the UK Center for Applied Energy Research, US DOE #DE-FC22-90PC90029 and by NSF Grant No. EHR-91-08764. The MIT authors greatfully acknowledge NSF grant No. DMR92-01878 and AFOSR Grant #AFOSR 93-0160 for support of their research.

REFERENCES

1. H. W. Kroto, J. R. Heath, S. C. O'Brien, R. F. Curl, and R. E. Smalley, Nature 318 (1985) 162.
2. *Accounts of Chemical Research*, 25 (1992)
3. M.S. Dresselhaus, G. Dresselhaus, R. Saito, and P.C. Eklund (Elsevier Science Publisher, 1992).
4. M.S. Dresselhaus, G. Dresselhaus, and P.C. Eklund, J. Mat. Res. 8, 2054 (1993).
5. K.-A. Wang *et al.*, Phys. Rev. B 45, 1955 (1992).
6. P. Zhou *et al.*, Phys. Rev. B 46, 2595 (1992).
7. Z.H. Dong *et al.*, Phys. Rev. B 48, 2862 (1993).
8. K. -A Wang *et al.*, Phys. Rev. B 48, 11375 (1993).
9. A.M. Rao *et al.*, Science 259, 955 (1993).
10. D.S. Cornett *et al.*, J. Phys. Chem. 97, 5036 (1993).
11. P. Zhou, Z.H. Dong, A. M. Rao, and P.C. Eklund, Chem. Phys. Lett. 211, 337 (1993).
12. Y. Wang *et al.*, Chem. Phys. Lett. 211, 341 (1993).
13. Y. Wang, J. M. Holden, X. X. Bi, and P. C. Eklund, Chem. Phys. Lett. (in press).
14. P. Heiney, J. Phys. Chem. Solids 53, 1333 (1992) .
15. W.I.F. David *et al.*, Europhys. Lett. 18, 219 (1992).
16. R. Tycko *et al.*, Phys. Rev. Lett. 67, 1886 (1991).
17. R.D. Johnson, D.S. Bethune, and C.S. Yannoni, Acc. Chem. Res. 25, 169 (1992).
18. P.A. Heiney *et al.*, Phys. Rev. Lett. 66, 2911 (1991) .
19. W.I.F. David *et al.*, Nature 353 (1991)
20. P. C. Eklund *et al.*, J. Phys. Chem. Solids 53, 1391 (1992).
21. G. Dresselhaus, M. S. Dresselhaus, and P. C. Eklund, Phys. Rev. B 45, 6923 (1992).
22. D.S. Bethune *et al.*, Chem. Phys. Lett. 179, 181 (1991).
23. W. Krätschmer, L. D. Lamb, K. Fostiropoulos, and D. R. Huffman, Nature 347, 354-358 (1990).
24. Narrow structure is also discerned in the IR spectrum over the range 1800 - 3000 cm-1 and has been reported in Ref. 8,
25. P. C. Painter, and J. L. Koenig, Spectrochim. Acta 33A, 1003 (1977).
26. P. Zhou *et al.*, Appl. Phys. Lett. 60, 2871 (1992) .
27. S. J. Duclos, R. C. Haddon, S. H. Glarum, and K. B. Lyons, Solid State Comm. 80, 481 (1991) .
28. S.H. Tolbert *et al.*, Chem. Phys. Lett. 188, 163 (1992).
29. M. Matus, and H. Kuzmany, Appl. Phys. A56, 241 (1993).
30. K. Akers, K. Fu, P. Zhang, and M. Moskovits, Science 259, 1152 (1993).
31. B. Chase, N. and Herron, and E. Holler, J. Phy. Chem. 96, 4262 (1992).
32. Y. Wang *et al.*, Phys. Rev. B 45, 14396 (1992).
33. A.M. Rao *et al.*, Phys. Rev. B. submitted (1994)
34. A. Ito, T. Morikawa, and T. Takahashi, Chem. Phys. Lett. 211, 333 (1993) .
35. H. Yamawaki *et al.*, J. Phys. Chem. 97, 11161 (1993).
36. M. Menon, K. R. Subbaswamy, and M. Sawtarie, Phys. Rev. B (in press).
37. K. Venkatesan & V. Ramamurthy, Photochemistry in organized and Constrained media 133 (1991) .
38. S. L. Ren *et al.*, Appl. Phys. Lett. 59, 2678 (1991).
39. J.W. Arbogast *et al.*, J. Phys. Chem. 95, 11-12 (1991).
40. R.R. Hung, and J.J. Grabowski, J. Physical Chem. 95, 6073-6074 (1991).
41. P.C. Eklund *et al.*, Mater. Sci. Eng. B 19, 154 (1993).
42. B. Birks, Photophysics of aromatic molecules, (Wiley- Interscience, London) (1970)
43. P.A. Lane *et al.*, Phys, Rev. Lett. 68, 887-890 (1992).
44. M.R. Wasielewski *et al.*, J. Am. Chem. Soc. 113, 2772-2776 (1991).